Efficient Analysis of Antennas Mounted on Electrically Large Complex Platforms

Nie Xiao Chun [1], Yuan Ning [1], Gan Yeow Beng [1], Wang Chao Fu [1] and Li Le Wei [2]

[1] *Temasekt Laboratories, National University of Singapore*
5 Sports Drive 2, Singapore 117508, tslniexc@nus.edu.sg
[2] *Department of Electrical and Computer Engineering, National University of Singapore*
10 Kent Ridge Crescent, Singapore 119260

Abstract

This paper presents an accurate and efficient method for the analysis of antennas mounted on electrically large complex platform. The Method of Moments (MoM) is applied to solve the problem and the precorrected-FFT algorithm is used to reduce memory requirement and speed up the computations. The effects on antenna parameters such as directivity, realised gain, radiation pattern, input impedance and radiation efficiency due to its environment are investigated. Several numerical examples are presented to verify the code and illustrate the capability of the present method.

1. Introduction

The behaviour of antennas mounted on aircraft or other complex platform, such as ship, satellite, *etc.* will be affected by mutual coupling between different antennas and interactions between antennas and supporting structures. To have better control on the electromagnetic compatibility (EMC) and reduce degradation in antenna performance due to environment, an accurate analysis of the antenna-platform system is required.

In this paper, an efficient method based on the surface-wire integral equation (SWIE) and precorrected-FFT (P-FFT) algorithm is presented for the analysis of monopole antennas on-board large complex platform. In this method, both the antenna and platform are included in the solution domain. The integral equation is set up by enforcing the boundary condition on the surface of the antenna and platform. Next, the Method of Moments (MoM) is used to solve the integral equation. The surface of the platform is modelled by a number of triangular patches, while the monopole antennas are modelled by linear segments. Triangular type basis functions are used to expand the unknown currents. An attachment mode is introduced at the junction of the antenna and the platform to consider the rapidly varying patch current in the vicinity. The precorrected-FFT method is used to reduce memory requirement and speed up the matrix-vector multiplications in the iterative solution. To further improve the efficiency of the method, the incomplete LU (ILU) pre-conditioner is employed for better convergence rate of the matrix system. The present method is capable of predicting the behaviour of the monopole antennas on board large complex platform efficiently and accurately.

2. Formulation

Consider a set of monopole antennas mounted on a large, perfect-electric-conducting (PEC) body. By invoking the equivalence principle, equivalent surface current $\boldsymbol{J}_S$ and wire current $\boldsymbol{J}_w$ are introduced on the surface of the PEC platform and the monopole antennas. To account for the continuity of the electric current from the monopole to the platform and the rapidly varying patch current at the transition from wire to surface, a junction current $\boldsymbol{J}_J$ is introduced on both the patch surface and the wire. The equivalent currents satisfy the following surface-wire integral equation:

$$\boldsymbol{E}^i_{\tan} = -\boldsymbol{E}^s_{\tan} \qquad on\ S_S \text{ and } S_W \tag{1}$$

where S_S and S_W are the surfaces of the platform and antennas, respectively.

The scattered field $\boldsymbol{E}^s$ is due to the combined contribution of the surface current $\boldsymbol{J}_S$, wire current $\boldsymbol{J}_w$, and junction current $\boldsymbol{J}_J$, which can be obtained from

$$\boldsymbol{E}^s(\boldsymbol{r}) = \sum_{\alpha} \left(-j\omega \boldsymbol{A}_\alpha(\boldsymbol{r}) - \nabla\Phi_\alpha(\boldsymbol{r})\right) \quad \alpha = S, W, J \tag{2}$$

where $A_\alpha(\boldsymbol{r})$ and Φ_α are the vector and scalar potential produced by current $\boldsymbol{J}_\alpha$. To solve Eq. (1), the conducting surfaces and wires are divided into triangular patches and linear segments, respectively. Next, the surface current $\boldsymbol{J}_S$, wire current $\boldsymbol{J}_w$, and junction current $\boldsymbol{J}_J$ are expanded using the Rao-Wilton-Glisson (RWG) basis functions [1], the triangular basis functions [2] and the junction basis functions [2], respectively. It should be noted that the junction basis function is defined on the junction region comprising a segment of the probe and a small area of the patch surface in the vicinity of the connection point. Using Galerkin's testing technique, the integral equation is converted into a matrix equation:

$$\begin{bmatrix} \boldsymbol{Z}^{S,S} & \boldsymbol{Z}^{S,W} & \boldsymbol{Z}^{S,J} \\ \boldsymbol{Z}^{W,S} & \boldsymbol{Z}^{W,W} & \boldsymbol{Z}^{W,J} \\ \boldsymbol{Z}^{J,S} & \boldsymbol{Z}^{J,W} & \boldsymbol{Z}^{J,J} \end{bmatrix} \begin{bmatrix} \boldsymbol{I}_S \\ \boldsymbol{I}_W \\ \boldsymbol{I}_J \end{bmatrix} = \begin{bmatrix} \boldsymbol{V}_S \\ \boldsymbol{V}_W \\ \boldsymbol{V}_J \end{bmatrix} \tag{3}$$

Elements of the sub-matrices $\boldsymbol{Z}^{\beta,\gamma}$ ($\beta,\gamma = S,W,J$) are given by

$$Z_{mn}^{\beta,\gamma} = j\omega \int_{S_m^\beta} \boldsymbol{f}_m^\beta \cdot \boldsymbol{A}_{mn}^\gamma d\beta - \int_{S_m^\beta} \Phi_{mn}^\gamma \nabla_s \cdot \boldsymbol{f}_m^\beta d\beta \tag{4}$$

where $\boldsymbol{A}_{mn}^\gamma$ and Φ_{mn}^γ are the contributions to $\boldsymbol{A}$ and Φ from a single basis function $\boldsymbol{f}_n^\gamma$, given by:

$$\boldsymbol{A}_{mn}^\gamma(\boldsymbol{r}) = \frac{\mu_0}{4\pi} \int_{\Sigma S_n^{\gamma\pm}} \boldsymbol{f}_n^\gamma(\boldsymbol{r}') \frac{e^{-jk_0|\boldsymbol{r}-\boldsymbol{r}'|}}{|\boldsymbol{r}-\boldsymbol{r}'|} d\boldsymbol{r}' \tag{5}$$

$$\Phi_{mn}^\gamma(\boldsymbol{r}) = -\frac{1}{4\pi j\omega\varepsilon_0} \int_{\Sigma S_n^{\gamma\pm}} \nabla \cdot \boldsymbol{f}_n^\gamma(\boldsymbol{r}') \frac{e^{-jk_0|\boldsymbol{r}-\boldsymbol{r}'|}}{|\boldsymbol{r}-\boldsymbol{r}'|} d\boldsymbol{r}' \tag{6}$$

The right-hand side vector $\boldsymbol{V}$ of Eq. (3) is the excitation of the antenna-platform system. In this paper, a delta-gap voltage source of 1V is assumed at the feed point of the driven antenna.

By solving the matrix equation (3), the unknown coefficients are obtained, from which various parameters of the on-board antennas can be calculated. However, the coefficient matrix $\boldsymbol{Z}$ is a dense and complex-valued matrix, requiring $O(N^2)$ storage, where N is the number of unknowns. A direct solution to Eq. (3) requires $O(N^3)$ operations and an iterative solution requires $O(N^{iter}N^2)$ operations, where N^{iter} is the number of iterations required to satisfy a predefined convergence criterion. Such requirements are computationally expensive and easily exceed the capacity of the latest computer. Fortunately, recently developed fast algorithms can be used to alleviate this problem. In this paper, we used the precorrected-FFT method [3] to speed up the matrix-vector multiplications in the iterations.

The P-FFT method considers the near- and far-zone interactions separately when evaluating a matrix-vector product, *i.e.*

$$\boldsymbol{Z} \cdot \boldsymbol{I} = \boldsymbol{Z}^{near} \cdot \boldsymbol{I} + \boldsymbol{Z}^{far} \cdot \boldsymbol{I} \tag{7}$$

The near-zone interactions are computed directly and stored while the far-zone interactions are obtained in an approximate but efficient way.

First, a uniform grid is introduced to enclose the entire solution domain, including the antennas and the platform. By matching the scalar or vector potentials due to the original source distributions in the support of the basis functions ($\boldsymbol{f}_n^\beta(\boldsymbol{r})$ and $\nabla \cdot \boldsymbol{f}_n^\beta(\boldsymbol{r})$ $\beta = S,W,J$) and that produced by the grid sources at some pre-selected test points, we can construct the projection operators

$$\boldsymbol{W}^\beta = \left[\boldsymbol{P}^{gt}\right]^+ \boldsymbol{P}^\beta, \quad \beta = S,W,J \tag{8}$$

where $\boldsymbol{P}^{gt}$ is the mapping between the grid sources and the test-point potentials, and $\boldsymbol{P}^\beta$ is the mapping between the original source distributions and the test-point potentials, respectively.

From the projection operators in Eq. (8), we can replace the original source distributions in the irregular mesh by a set of equivalent point sources on a uniform grid. Thus, the relationship between the potentials at the grid points and the grid sources is in fact a convolution, which can be rapidly calculated using the discrete Fast Fourier Transforms (FFTs). Upon computing the grid potentials, the potentials on the original elements are obtained via interpolation. The transpose of the projection operators can be used as the interpolation operators. The grid approximation of the sub-matrix in Eq. (3) can be written as

$$\tilde{\boldsymbol{Z}}^{\alpha,\beta} = \boldsymbol{W}^{\alpha^T} \boldsymbol{H} \boldsymbol{W}^\beta \tag{9}$$

where $\boldsymbol{H}$ represents the convolution operators. Finally, the errors introduced in the nearby interactions by the grid approximation should be removed. Next, the sub-matrix obtained by the P-FFT method is given by the following formula

$$\hat{\boldsymbol{Z}}^{\alpha,\beta} = \tilde{\boldsymbol{Z}}^{\alpha,\beta} + (\boldsymbol{Z}^{\alpha,\beta} - \boldsymbol{W}^{\alpha^T} \boldsymbol{H} \boldsymbol{W}^\beta) \qquad \alpha,\beta = S,W,J \tag{10}$$

where the second term on the right of Eq. (10) is the so–called pre-correction operator. It is required only when the distance between the basis function $\boldsymbol{f}_n^\beta$ and the testing function $\boldsymbol{f}_m^\alpha$ is less than a predefined threshold; otherwise, it is set to zero.

Using the above three sparse operators (projection, interpolation and the pre-correction) and one global operator (convolution), the matrix-vector multiplications can be speed up significantly, with reduction in memory requirement.

3. Numerical Examples

The first test case considered is as shown in Fig.1. A monopole is located at the center of an edge of a rectangular box, and a parasitic monopole is located at the center of the opposite edge of the same box. The radius and length of the monopole are 1mm and 25cm, respectively. The rectangular box has a length and width of 1.8m and a height of 20cm. Fig. 2 shows the calculated self admittance of the driven monopole and the mutual admittance between the two monopoles as a function of frequency. The results obtained by the Method of Moments in [4] are also shown in the figure for comparison. Good agreement is observed, validating the present method.

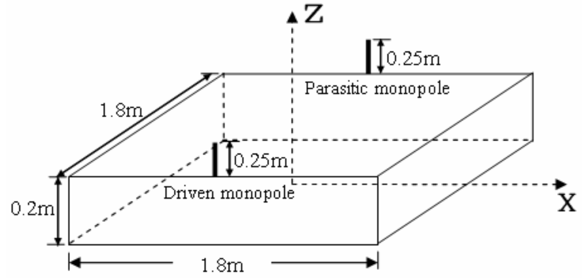

Fig. 1 Geometry of two monopole antennas mounted on a rectangular box

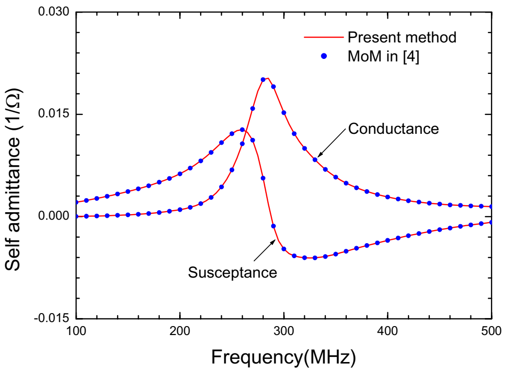

(a) Self admittance of the driven monopole

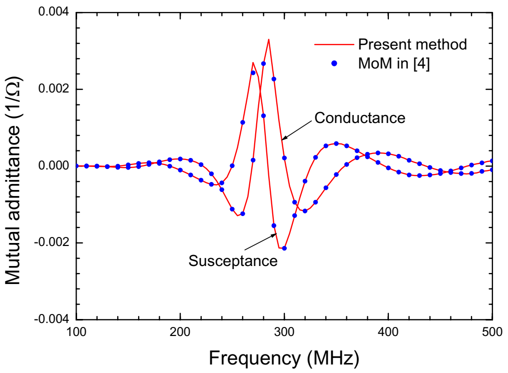

(b) Mutual admittance between the two monopoles

Fig. 2 Variation of the self and mutual admittance with frequency

The second test case is as shown in Fig.3. A 25cm-long monopole antenna tilting at 41° from the z axis in the yoz plane is mounted on the rear section of an aircraft model. The rear section model is derived from a full aircraft model, but with the truncated end terminated by a PEC plane. In this test case, the antenna is located at a disadvantageous position. The coupling between the antenna and the aircraft is very complicated, and the presence of the edges will affect the performance of the antenna significantly. Accurate results cannot be obtained without all interactions taken into account. Therefore, the full wave low frequency method is deemed to be suitable to handle this problem accurately.

The directive pattern of the on-board monopole antenna at 300MHz in the yoz plane and xoy plane are shown in Fig. 4 and Fig.5, respectively. The results obtained from the commercial software FEKO based on the MoM and parallel processing are also shown in the figures for comparison. It is observed that the results from the two methods agree very well, except for the cross-polarized pattern in the yoz plane. This is reasonable since the cross-polarized pattern in the yoz plane is about 40 dB below the co-polarized pattern and cannot be computed accurately. In the simulation, the surface of the platform is discretized into 14,828 triangle patches, while the monopole is divided into 20 segments, resulting in a total of 22,262 unknowns. A 50Ω load terminates the feed point of the monopole.

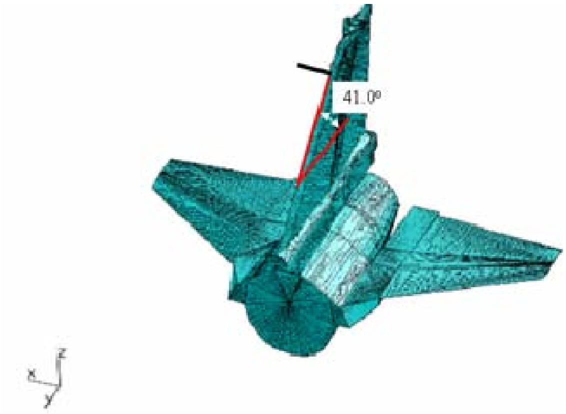

Fig.3 Geometry of a monopole antenna mounted on the rear section of an aircraft model

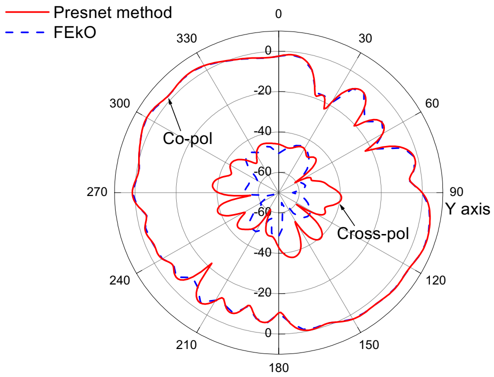

Fig.4 Directive pattern of the monopole antenna in the yoz plane

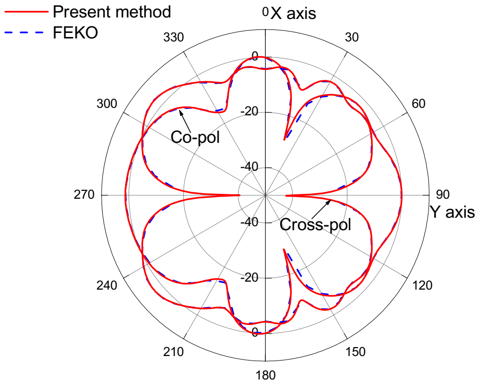

Fig.5 Directive pattern of the monopole antenna in the xoy plane

We have also compared other antenna parameters obtained by the present method with that from FEKO. The comparison of the input impedance, radiation efficiency and total output power is shown in Table 1. Again, good agreements are observed.

TABLE 1: COMPARISONS OF ANTENNAS PARAMETERS OBTAINED BY THE PRESENT METHOD AND THE FEKO

Method	Input Impedance (Ω)	Efficiency (%)	Total output Power (mw)
Present method	96.04+j39.87	65.76	3.186
FEKO	91.69+j46.21	64.71	3.190

To show the efficiency of the incomplete LU (ILU) pre-conditioner, we compared the convergence rate of the system with and without pre-conditioning. The normalized residual norms (NRN) as a function of the number of iterations for these two cases are shown in Fig.6. It is observed that without pre-conditioner, the solution converges to a NRN of 1% after 700 iterations. However, after pre-conditioning, a NRN of 0.01% can be attained with only 74 iterations. Detailed implementation of the ILU pre-conditioner can be found in [5]. For this test case, our code required 533MB of memory and took about 45.2 minutes to obtain the final solution on a Pentium 2.4G PC. The paralleled FEKO operates on a workstation with 16 processors (Intel® Xeon™ MP CPU 3.16GHz). The total CPU time of all processors is 26,502 seconds and the peak memory usage for all processors is 7.48GB.

Finally, the frequency response of the reflection coefficient at the feed point is obtained as shown in Fig. 7. It is observed that the resonant frequency of the monopole shifts from 300MHz to 272MHz due to the interactions between the monopole and the platform.

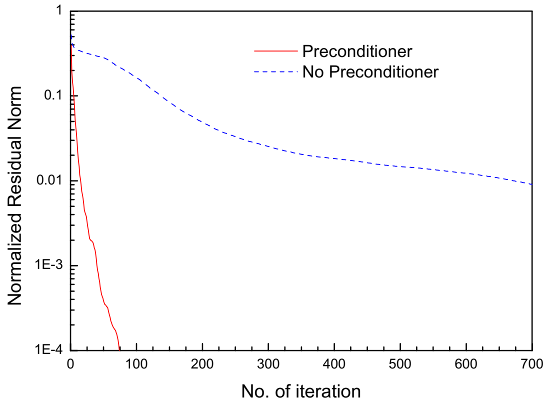

Fig.6 Convergence comparison of the solution with and without the ILU pre-conditioner

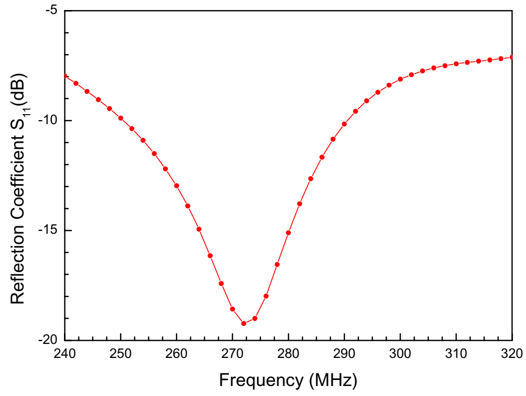

Fig. 7 Frequency response of the reflection coefficient at the feed-point of the monopole

4. Conclusions

The surface-wire integral equation approach accelerated by the preconditioned-FFT method is used to analyze monopole antennas on board electrically large complex platforms. The method significantly reduces the memory requirement and CPU time, enabling the modelling of large problems with limited computer resources. Although only monopole antennas are considered in this paper, the present method is not restricted to this application. Extension of the method to other types of antennas mounted on large platform is straightforward.

References

[1] Rao S.M., D.R. Wilton, and A.W. Glisson, “Electromagnetic scattering by surfaces of arbitrary shape,” *IEEE Trans. Antennas Propagat.*, vol.30, no.3, pp.409-418, May, 1982

[2] S.U. Hwu, D.R. Wilton, and S.M. Rao, “Electromagnetic scattering and radiation by arbitrary conducting wire-surface configuration,” *IEEE APS Int. Symp. Dig.*, pp.890-893, 1988

[3] N. Yuan, T.S. Yeo, X.C. Nie, Y.B. Gan and L.W. Li, “Analysis of probe-fed conformal microstrip antennas on finite ground substrate”, *IEEE Trans. Antennas Propagat.*, vol. 54, no. 2, pp. 554-563, Feb. 2006

[4] X.C. Wei and E.P. Li, “Wide-band EMC analysis of on-platform antennas using impedance matrix interpolation with the moment method-physical optics method,” *IEEE Trans. Electromagnetic Compatibility*, vol.45, no.3, pp.553-556, Aug. 2003

[5] Y. Saad, “ILUT: a dual threshold incomplete LU factorozation,” *Numer. Linear Algebra Appl.*, vol.1, no.4, pp.387-402, 1994.